

Prognostic Accuracy of Cerebral Blood Flow Measurement by Perfusion Computed Tomography, at the Time of Emergency Room Admission, in Acute Stroke Patients

Max Wintermark, MD,¹ Marc Reichhart, MD,² Jean-Philippe Thiran, PhD,³ Philippe Maeder, MD,¹ Marc Chalaron, MD,¹ Pierre Schnyder, MD,¹ Julien Bogousslavsky, MD,² and Reto Meuli, MD, PhD¹

The purpose of this study was to determine the prognostic accuracy of perfusion computed tomography (CT), performed at the time of emergency room admission, in acute stroke patients. Accuracy was determined by comparison of perfusion CT with delayed magnetic resonance (MR) and by monitoring the evolution of each patient's clinical condition. Twenty-two acute stroke patients underwent perfusion CT covering four contiguous 10mm slices on admission, as well as delayed MR, performed after a median interval of 3 days after emergency room admission. Eight were treated with thrombolytic agents. Infarct size on the admission perfusion CT was compared with that on the delayed diffusion-weighted (DWI)-MR, chosen as the gold standard. Delayed magnetic resonance angiography and perfusion-weighted MR were used to detect recanalization. A potential recuperation ratio, defined as $PRR = \text{penumbra size} / (\text{penumbra size} + \text{infarct size})$ on the admission perfusion CT, was compared with the evolution in each patient's clinical condition, defined by the National Institutes of Health Stroke Scale (NIHSS). In the 8 cases with arterial recanalization, the size of the cerebral infarct on the delayed DWI-MR was larger than or equal to that of the infarct on the admission perfusion CT, but smaller than or equal to that of the ischemic lesion on the admission perfusion CT; and the observed improvement in the NIHSS correlated with the PRR (correlation coefficient = 0.833). In the 14 cases with persistent arterial occlusion, infarct size on the delayed DWI-MR correlated with ischemic lesion size on the admission perfusion CT ($r = 0.958$). In all 22 patients, the admission NIHSS correlated with the size of the ischemic area on the admission perfusion CT ($r = 0.627$). Based on these findings, we conclude that perfusion CT allows the accurate prediction of the final infarct size and the evaluation of clinical prognosis for acute stroke patients at the time of emergency evaluation. It may also provide information about the extent of the penumbra. Perfusion CT could therefore be a valuable tool in the early management of acute stroke patients.

Ann Neurol 2002;51:417-432

Stroke is the third-leading cause of death in the United States, after cardiovascular disease and cancer. Each year in the United States, it affects 730,000 to 760,000 patients, a third of whom will be permanently disabled, and thus represents the leading cause of disability in the country.^{1,2} Thrombolysis has been introduced as a new therapy for acute stroke,³ but present indications for intravenous thrombolytic therapy depend on the time interval since the onset of symptoms (less than 3 hours) and noncontrast cerebral computed tomography (CT) findings (absence of cerebral hemorrhage and extent of the cerebral hypodensity).^{1,3,4} Evaluation of brain perfusion prior to thrombolysis has been suggested as a possible selection criterion for treatment,

since extensive infarct and little salvageable penumbra in the territory of an occluded middle cerebral artery (MCA) seem to be linked to an unfavorable risk-benefit ratio.⁴⁻⁹ The aim of thrombolysis is to save ischemic but still-viable cerebral parenchyma.¹⁰

Viability of the cerebral parenchyma depends on the cerebral blood flow (CBF).¹¹⁻¹³ Multiple thresholds describing the progressive inhibition of the electrical and metabolic activity of neurons have been defined in various animal species.¹³⁻¹⁵ Soon after cerebral arterial occlusion, reversible inhibition or penumbra occurs in the cerebral parenchyma territory that is usually perfused by this artery; then, starting from the center of the arterial territory, infarct progressively replaces pen-

From the Departments of ¹Diagnostic and Interventional Radiology and ²Neurology, CHUV, Lausanne, Switzerland, and the ³Signal Processing Laboratory, Swiss Federal Institute of Technology, Lausanne, Switzerland.

Received Mar 12, 2001, and in revised form Jul 30 and Nov 26. Accepted for publication Nov 29, 2001.

Address correspondence to Dr Bogousslavsky, Department of Neurology, CHUV-BH10, 1011 Lausanne, Switzerland.
E-mail: Julien.Bogousslavsky@chuv.hospvd.ch

umbra at a rate that depends on the degree of collateral circulation.^{13–18}

An additional major difference between cerebral penumbra and infarct relates to cerebral perfusion autoregulation. Complex autoregulation processes ensure both the adjustment of regional cerebral blood flows (rCBF) to local neuronal activity and CBF stability, despite changes in systemic arterial pressure. Vascular autoregulation in the brain causes vascular dilatation when the systemic pressure falls, thus maintaining a constant CBF. This vascular dilatation leads, in turn, to an increased regional cerebral blood volume (rCBV), which some authors equate with penumbra.^{19–23} In infarcted cerebral parenchyma, the autoregulation mechanisms are altered, and both the rCBF and rCBV are usually decreased.^{8,9} Penumbra and infarct maps can thus be inferred from rCBV and rCBF maps and could perhaps be used as an additional criterion to decide whether an acute stroke patient should be included in a thrombolysis protocol, since thrombolysis performed on patients with extensive cerebral infarct and a limited penumbra would not only be of little benefit, but also increase the risk of intracranial bleeding.^{8–10}

Perfusion Computed Tomography Technology

Various imaging techniques are now available to evaluate brain perfusion; these include perfusion CT.

Perfusion CT is a modern imaging technique that allows accurate quantitative assessment of rCBF and rCBV.^{24–26} It can be performed on acute stroke patients, since it involves only the sequential acquisition of cerebral CT images performed in cine mode during the intravenous administration of iodinated contrast material. It is well tolerated and not time-consuming, and can be integrated into the cerebral CT survey undergone by all stroke patients.^{24–27} Except for dedicated software, no special equipment is required. Perfusion CT data consist of contrast enhancement profiles obtained in each pixel; these profiles are linearly related to the time-concentration curves for the contrast material. Analysis of these curves is performed according to the central volume principle, which is reported to give the most accurate results for low injection rates of iodinated contrast material.^{28–33} The rCBV map is calculated from a quantitative estimation of the partial size averaging effect, which is completely absent in a reference pixel at the center of the large superior sagittal venous sinus.^{34–38} The impulse function and the related mean transit time (MTT) maps result from a deconvolution of the parenchymal time-concentration curves by a reference arterial curve. Finally, the rCBF value can be calculated from the rCBV and MTT values for each pixel using the following simple equation:^{31,32}

$$rCBF = \frac{rCBV}{MTT}$$

Hypotheses

Our purpose was to perform perfusion CT on acute stroke patients at the time of emergency room admission; to define rCBV, MTT, and rCBF maps; and to calculate penumbra and infarct maps according to the above-described principles. Assuming that thrombolysis can salvage the penumbra but not the infarct,¹⁰ we tried to answer two questions:

- (1) *What is the accuracy of admission perfusion CT in predicting infarcted cerebral areas?* We tried to answer this question by comparing the admission perfusion CT results with the final size of the cerebral infarct defined by delayed diffusion-weighted magnetic resonance (DWI-MR). DWI-MR does not provide information on the rCBF, but rather on the functional condition of cerebral neurons (microscopic proton diffusion, altered, for example, by cytotoxic edema), and has been shown to be accurate in the delineation of the nature and size of brain ischemia and in the quantification of tissue in the moderate-to-advanced stages of injury.⁸ In order to avoid pitfalls related to biphasic phenomena,^{39,40} DWI-MR performed a few days after the stroke was chosen as the reference for the final cerebral infarct size.
- (2) *What is the potential predictive value of the relative sizes of the penumbra and infarct in terms of clinical improvement?* Clinical improvement was evaluated on admission and a median of 1 month later (interquartile range, 0.825–1.625 months) using the National Institutes of Health Stroke Scale (NIHSS), which has been proven to provide an accurate assessment of stroke severity.^{41–43} We hypothesize that, in a patient with an extensive infarct and a relatively small penumbra, thrombolysis would salvage little and clinical improvement would be poor. On the other hand, in a patient with an extensive penumbra and a small infarct, recanalization of the occluded cerebral artery would lead to greater clinical improvement.

Patients and Methods

Patients

Our series consisted of 22 adults (13 men and 9 women; average age, 63 years; age range, 31–85 years) with an acute ischemic stroke diagnosed on the basis of clinical and non-contrast CT data. These patients were prospectively identified in the Emergency Department of our institution during the period of March to December 2000. The patients' char-

acteristics, the exact location of the ischemic stroke, use of thrombolysis, and recanalization of the occluded cerebral artery are summarized in Table 1.

In all 22 patients, noncontrast baseline cerebral CT was immediately followed by perfusion CT, this being part of the initial routine survey of acute stroke patients at our institution. Twelve of the patients also underwent a cerebral and cervical angio-CT. Eight of the 22 patients were eligible for intravenous thrombolytic therapy. Thrombolysis was begun at a median of 3 hours (interquartile range, 2.625–3 hours) after the stroke onset. No complications, particularly no hemorrhages, occurred in the 8 thrombolysed patients; but 15 days after the stroke onset, 1 patient died of septicemia following pulmonary infection.

After a median of 3 days (interquartile range, 3–4 days; median [interquartile range], 3 [3–4.75] days for the thrombolysis group and 3 [2.25–3] days for the nonthrombolysis group; $p = 0.209$) after admission, an MR examination, including T2 and DWI series, as well as cerebral and cervical angio-MR, were performed on each of the 22 patients.

In addition to the admission CT and delayed MR, two patients underwent a second cerebral CT survey before the MR. These sequential perfusion CT and MR examinations demonstrated the evolution of the penumbra over time, with and without arterial recanalization (Figs 1 and 2).

The time intervals between stroke onset and admission to the emergency room, perfusion CT, beginning of thrombolysis, and delayed MR were recorded. The permeability of the cerebral and cervical vessels was assessed from the admission angio-CT and delayed angio-MR.

In the surviving 21 patients, the NIHSS, Barthel index,

and modified Rankin scale were used to evaluate clinical condition both at the time of admission and after a median of 1 month (interquartile range, 0.825–2.625 months) (median [interquartile range], 1.4 [1.075–2.875] months for the thrombolysis group and 1 [0.475–1.325] month for the nonthrombolysis group; $p = 0.298$). The improvement in the NIHSS between admission and at a median of 1 month (interquartile range, 0.825–2.625 months) was used to evaluate clinical improvement.

For the patient who died of septicemia 15 days after stroke onset, a delayed MR was performed on day 5 and was included in the comparison with admission perfusion CT. The patient was assigned delayed Barthel and modified Rankin indices of 0 and 6, respectively. However, this patient was not included in the comparison of NIHSS improvement, which would have given a negative value (19 on admission and 42 in the final function outcome analysis).

Imaging Techniques

The perfusion CT examination consisted of two 40-second series separated by 5 minutes, each series consisting of one image per second in cine mode during intravenous administration of iodinated contrast material. The acquisition parameters for both series were 80kVp and 100mA.⁴⁴ For each series, CT scanning was initiated 7 seconds after injection of 50ml of iohexol (300mg/ml of iodine; Accupaque 300, Nycomed, Oslo, Norway) at a rate of 5ml per second into an antecubital vein using a power injector (CT9000; Libel-Flarsheim Company, Cincinnati, OH). The delay before the arrival of the contrast material allowed baseline images with-

Table 1. Characteristics of the 22 Patients with Acute Stroke Who Underwent Both Admission Perfusion CT and Delayed MR

Patient no.	Age (yrs)	Gender	Location of the Ischemic Stroke on the DWI-MR	Thrombolysis	Recanalization of the Occluded Cerebral Artery
1	68	M	Superficial posterior left MCA	No	Yes
2	54	M	Left MCA	Yes	Yes
3(†)	84	F	Superficial and deep left MCA	Yes	Yes
4	51	F	Superficial left MCA	No	Yes
5	51	F	Deep posterior right MCA	No	Yes
6	76	F	Superficial anterior right MCA	No	Yes
7	46	F	Posterior right MCA	No	No
8	78	M	Basilar artery	Yes	Yes
9	71	M	Superficial posterior left MCA	Yes	Yes
10	71	M	Posterior left MCA	Yes	Yes
11	61	M	Superficial right MCA	Yes	No
12	43	F	Left MCA	No	No
13	31	M	Anterior right MCA	No	No
14	50	M	Posterior left MCA	No	Yes
15 (see Fig. 1)	74	F	Anterior right MCA	No	Yes
16	85	F	Superficial anterior left MCA	No	No
17	68	M	Superficial left MCA	Yes	Yes
18	75	M	Right MCA	Yes	No
19	33	M	Right MCA	No	No
20	80	F	Right MCA	No	Yes
21	61	M	Posterior right MCA	No	Yes
22 (see Fig. 2)	83	M	Left MCA	No	No

†Deceased.

CT = computed tomography; DWI-MR = diffusion-weighted magnetic resonance; MCA = middle cerebral artery.

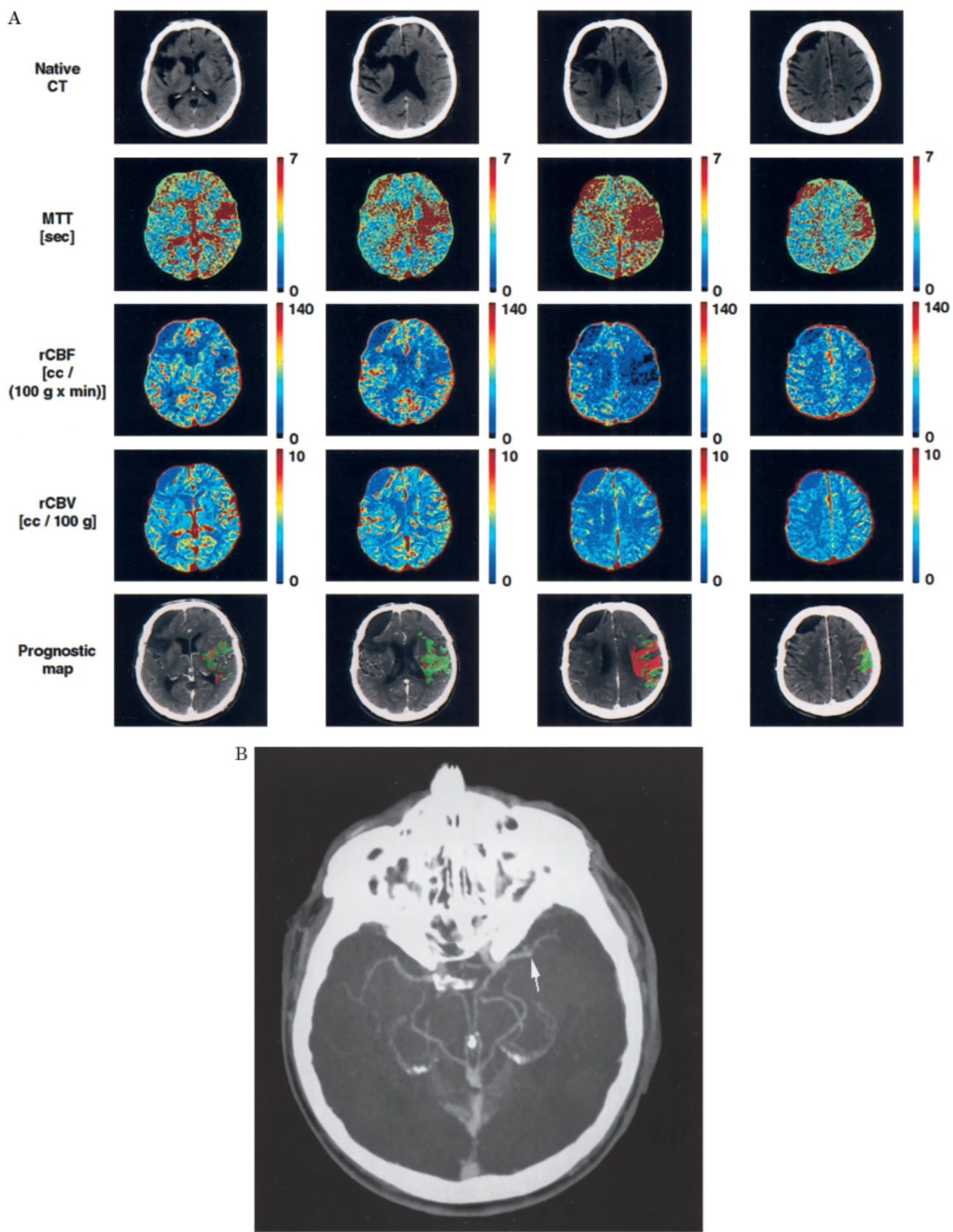


Figure 1

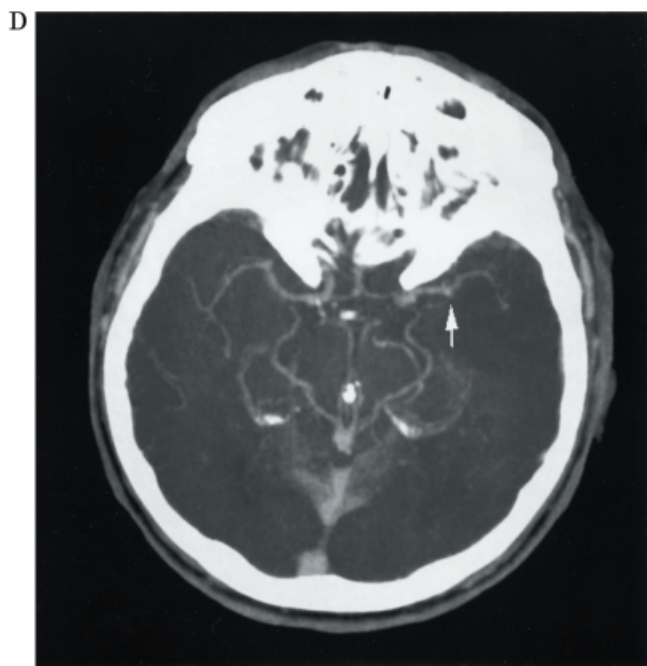
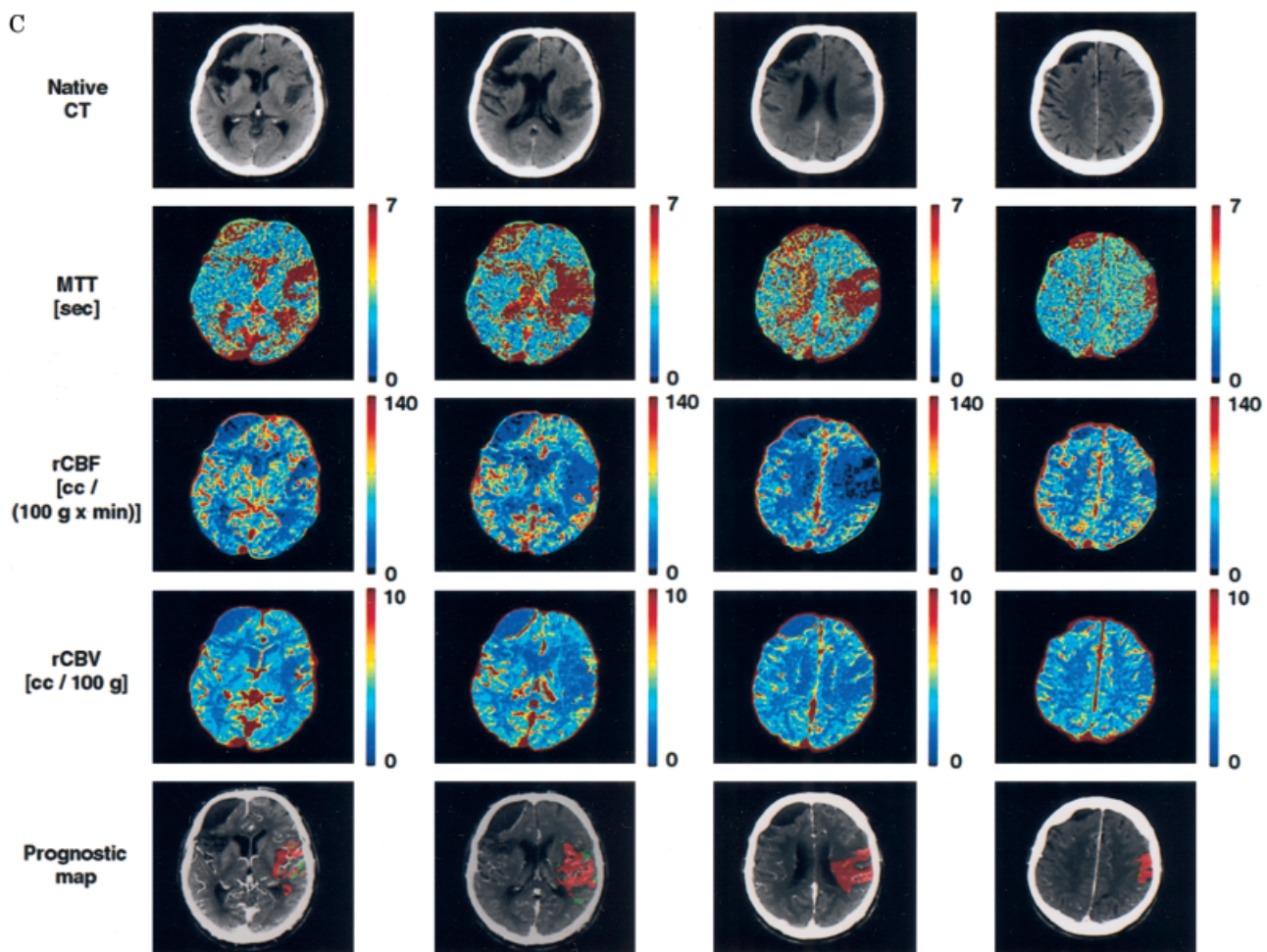


Figure 1 (Continued)

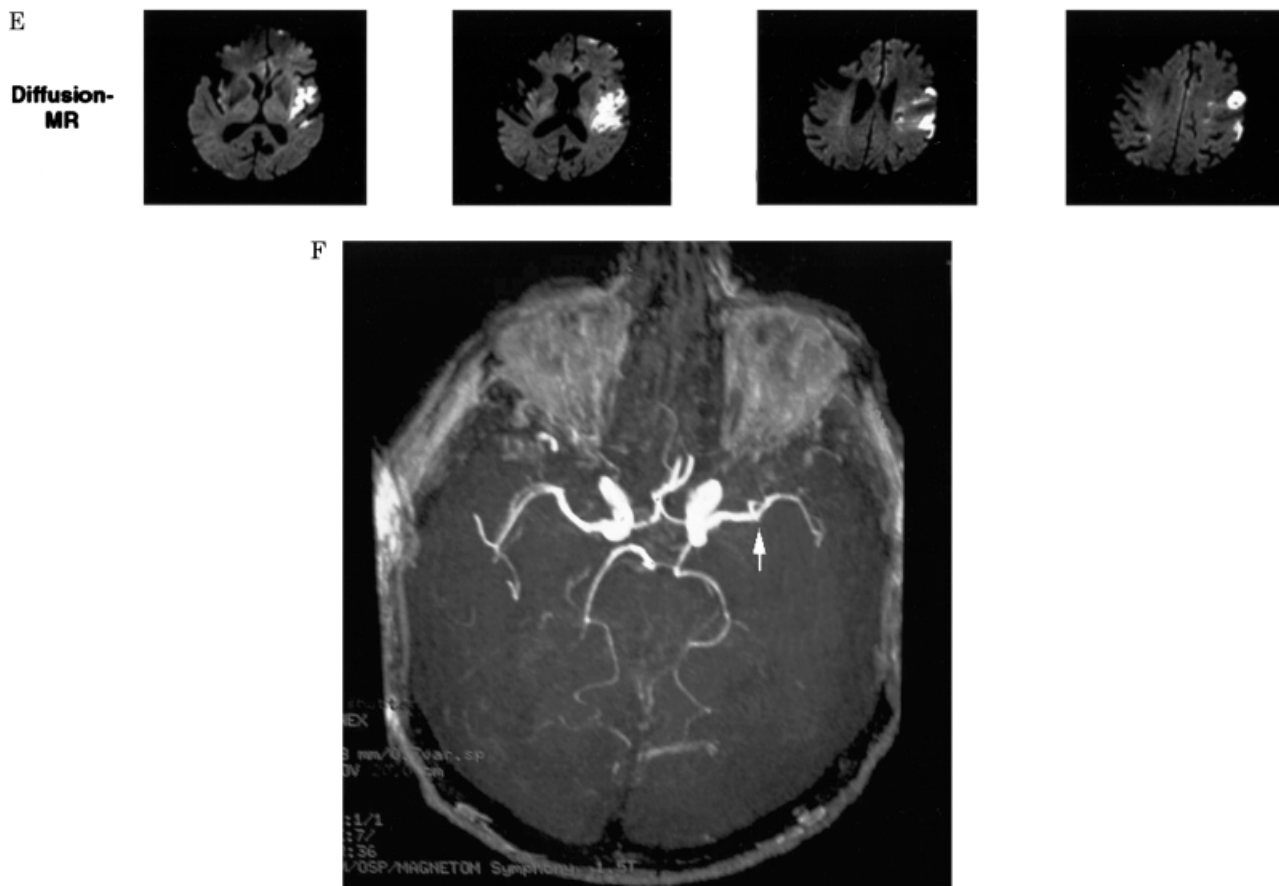


Fig 1. (Continued) Progression of the infarct over the penumbra in a case of persistent cerebral arterial occlusion. The patient was a male age 83 years with suspected anterior left sylvian artery stroke. (A) The noncontrast cerebral computed tomography (CT) (first line) obtained at the time of emergency room admission, 7 hours after stroke onset, showed an old right frontal lesion and slight left insula ribbon sign, whereas the more sensitive perfusion CT prognostic map (fifth line) identified a deep left middle cerebral artery (MCA) ischemia, with an infarct (red) component located on the left semioval center and a penumbra (green) lying on the left internal capsula, insula, and parietal operculum. The mean transit time (MTT) (second line) and regional cerebral blood flow (rCBF) (third line) were increased and decreased, respectively, in both the infarct and penumbra, whereas the regional cerebral blood volume (rCBV) (fourth line) was decreased in the infarct and either preserved or increased in the penumbra, due to autoregulation processes. (B) The admission angio-CT maximum intensity projection (MIP) displayed the occluded left MCA responsible for the reported cerebral ischemia. No thrombolysis was performed due to the time delay. (C) Worsening of the clinical condition justified the performance of a second CT 28 hours after the first. The noncontrast cerebral CT (first line) demonstrated a cerebral infarct in the exact location reported on the first perfusion CT. The perfusion CT prognostic map (fifth line) disclosed almost complete replacement of the first perfusion CT penumbra (green) by infarct (red). (D) The second angio-CT explained these findings by persistent occlusion of the left MCA. (E) Six days after admission, diffusion-weighted magnetic resonance (DWI-MR) demonstrated the cerebral infarct, which closely correlated with that described on the second perfusion CT prognostic map. (F) The persistent occlusion of the left MCA was confirmed by angio-MR.

out contrast enhancement to be acquired. Multidetector-array technology (Lightspeed CT unit; General Electric, Milwaukee, WI) allowed the acquisition of data from two adjacent 10mm sections for each series. The two perfusion CT series thus allowed the acquisition of data for four adjacent 10mm cerebral CT sections. The four studied cerebral sections were chosen above the orbits to protect the lenses, passing through the basal nuclei, then towards the vertex.

The cerebral and cervical angio-CT were performed using the parameters 120kVp, 240mAs, slice thickness 2.5mm,

slice acquisition interval 2mm, pitch 1.5:1, HS mode, intravenous administration of 50ml of iodinated contrast material at a rate of 3ml per second, and an acquisition delay of 10 seconds. Data acquisition was performed from the origin of the aortic arch branch vessels to the circle of Willis.

After a median of 3 days (interquartile range, 3–4 days) (median [interquartile range], 3.5 [3–4.75] days for the thrombolysis group and 3 [2.25–3] days for the nonthrombolysis group; $p = 0.209$) after admission, an MR examination was performed on all 22 patients using a 1.5T MR unit

(Symphony MR unit; Siemens, Erlangen, Germany). This included spin-echo T2-weighted series and DWI series (echoplanar spin-echo, TR = 5,000msec, TE = 100msec, b = 1,000, 20 5mm thick slices with a 1.5mm gap, matrix size = 128 × 128). Angio-MR was performed using a time-of-flight multislab 3-D FLASH technique for cerebral and cervical vessels. A 3-D FISP technique during the intravenous administration of a bolus of gadolinium was also used for cervical vessels.

This study protocol was approved by our review board, and institutional informed consent guidelines were followed.

Data Processing

The perfusion CT data were transferred to an SG1 Onyx workstation (Silicon Graphics, Mountain View, CA) and analyzed using perfusion analysis software to create parametric maps of rCBV, MTT, and rCBF. The penumbra and infarct maps calculated as follows: An ischemic cerebral area (penumbra + infarct) was defined as including cerebral pixels with a greater than 34% decrease in rCBF compared with the corresponding region in the cerebral hemisphere, defined as healthy on the basis of clinical symptomatology. In this selected area, 2.5ml per 100g was chosen as the rCBV threshold, in agreement with published data suggesting that cerebral parenchyma below this rCBV level is highly likely to die.^{13,19,20,49–51} Again, within this selected area, pixels with rCBV values higher or lower than 2.5ml per 100g were attributed, respectively, to the penumbra or the infarct. The resultant cerebral penumbra and infarct maps were combined and graphically displayed as a prognostic map, with the infarct shown in red and the penumbra in green (see Figs 1 and 2). Four cerebral sections in the DWI-MR sequence were selected as corresponding most closely to the chosen perfusion CT sections. The infarcted cerebral area on the DWI-MR images was defined as including all pixels above an intensity threshold, in order to exclude the contralateral hemisphere and choroidal plexi from the infarcted area, since the stroke was unilateral in all 22 patients.

Data Analysis

For each patient, the final results included four perfusion CT penumbra maps, four perfusion CT infarct maps, and four

DWI-MR infarct maps (see Figs 1 and 2). The DWI-MR sections examined were selected at approximately the same level as the perfusion CT sections. Analysis of perfusion CT infarct and penumbra maps was performed in two ways:

- (1) The perfusion CT infarct and penumbra maps were first used to measure the size of the predicted infarcted area in cm². The size of the final infarcted area was measured on the corresponding sections of the DWI-MR, regarded as the gold standard for statistical analysis. Linear regression analysis and bilateral T-tests for matched variables were used to compare infarct sizes on the corresponding sections of the perfusion CT and DWI-MR. Statistically significant *p* values were lower than 0.05.
- (2) The perfusion CT penumbra and infarct maps were used to calculate a potential recuperation ratio (PRR), using the following equation;

$$\text{PRR} = \frac{\text{penumbra size}}{\text{penumbra size} + \text{infarct size}}$$

A PRR was determined for each of the four slices and a mean PRR calculated for each patient.

Correlations between the admission NIHSS and the size of the ischemic cerebral area on the admission perfusion CT; among the infarct sizes on the delayed DWI-MR and the delayed NIHSS, Barthel index, and modified Rankin score; and between the NIHSS improvement and the PRR were evaluated by linear regression analysis, with calculation of Pearson's linear correlation coefficients.

Results

Time Delays

The median time from stroke onset to emergency room admission was 1.875 (interquartile range, 1.5–4.875) hours (median [interquartile range], 1.5 [1.5–1.5] hours for the thrombolysis group and 4.5 [2.875–6] hours for the nonthrombolysis group; *p* = 0.009),

Fig 2. Recovery of the penumbra in a case of cerebral arterial recanalization. The patient was a female age 74 years with anterior right sylvian artery stroke suspected on the basis of the physical examination 5 hours after symptomatology onset. (A) The noncontrast cerebral computed tomography (CT) obtained at the same time (first line) demonstrated a subtle corticomedullar dedifferentiation on the head of the right caudate nucleus, whereas the more sensitive perfusion CT prognostic map (second line) clearly identified a deep right middle cerebral artery (MCA) ischemia, with an infarct (red) component located on the head of the right caudate nucleus and a penumbra (green) lying on the right internal capsula and lenticulate nucleus. (B) Admission angio-CT maximum intensity projection displayed the occluded right MCA responsible for the reported cerebral ischemia. No thrombolysis was performed due to the time delay. The evolution of the clinical condition was favorable, but a generalized seizure occurred 7 hours after the first CT, which justified the performance of a second CT (C) to rule out a reperfusion hemorrhage. The noncontrast cerebral CT (first line) did not display any extension of the ischemic territory depicted in (A). The perfusion CT prognostic map (second line) showed limited progression of the infarct (red) over the first perfusion CT penumbra, whereas the penumbra (green) had mostly resolved. (D) The second angio-CT explained these findings by right MCA recanalization, which occurred some time after the first CT; this time delay allowed for the observed progression of the infarct. Immediately after recanalization, infarct progression over the penumbra was stopped and the residual penumbra recovered. (E) Three days after admission, diffusion-weighted magnetic resonance (DWI-MR) demonstrated the residual infarct, which closely correlated with that described on the second perfusion CT prognostic map. (F) Right MCA recanalization was again demonstrated by delayed angio-MR.

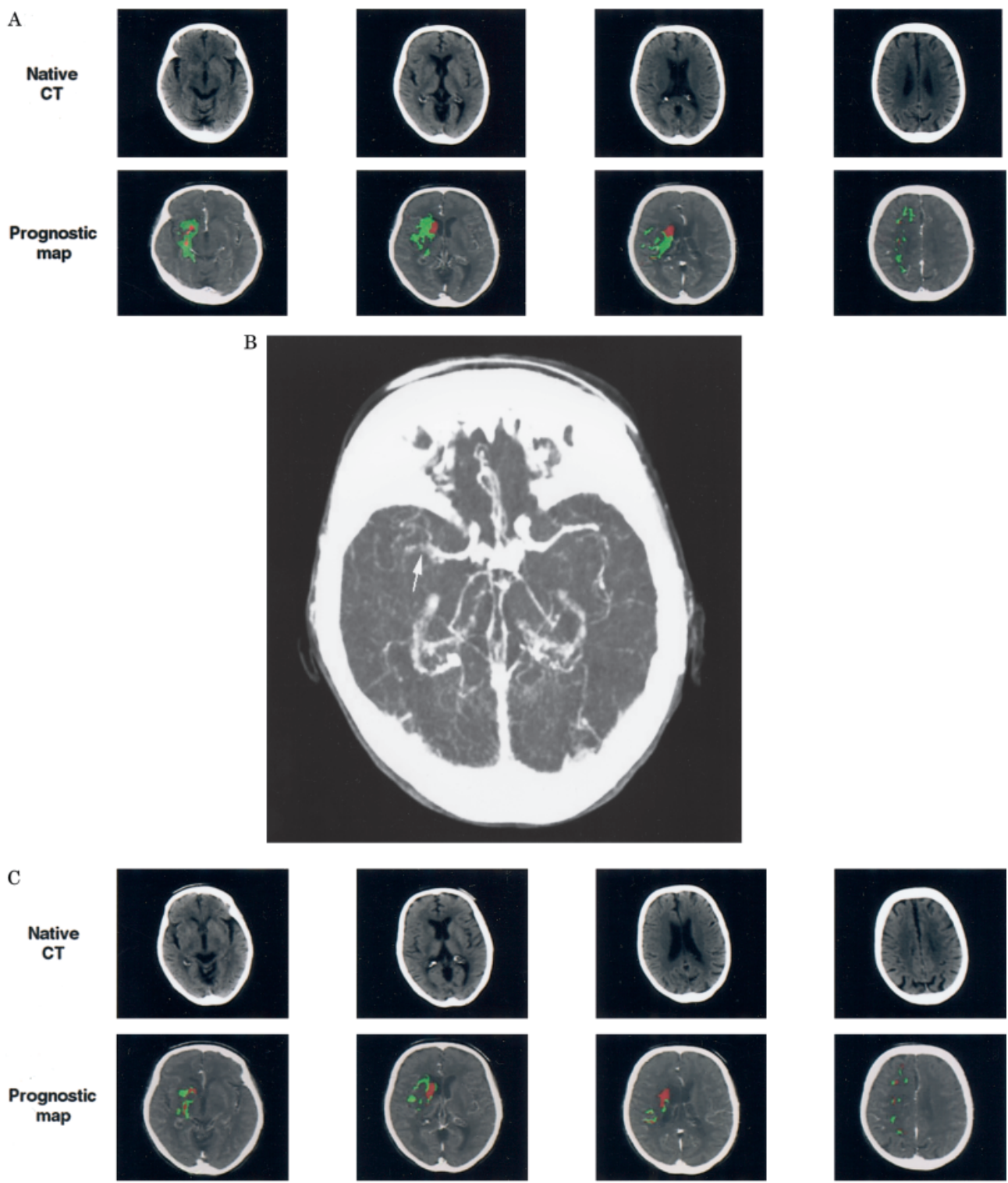


Figure 2

while the median time from stroke onset to perfusion CT scanning was 3.25 (2–6) hours (median [interquartile range], 2 [2–2] hours for the thrombolysis group and 6 [3.25–8] hours for the nonthrombolysis

group; $p = 0.010$). The perfusion CT examinations were well tolerated by all 22 patients and added only 10 minutes to the time required for the admission cerebral CT survey.

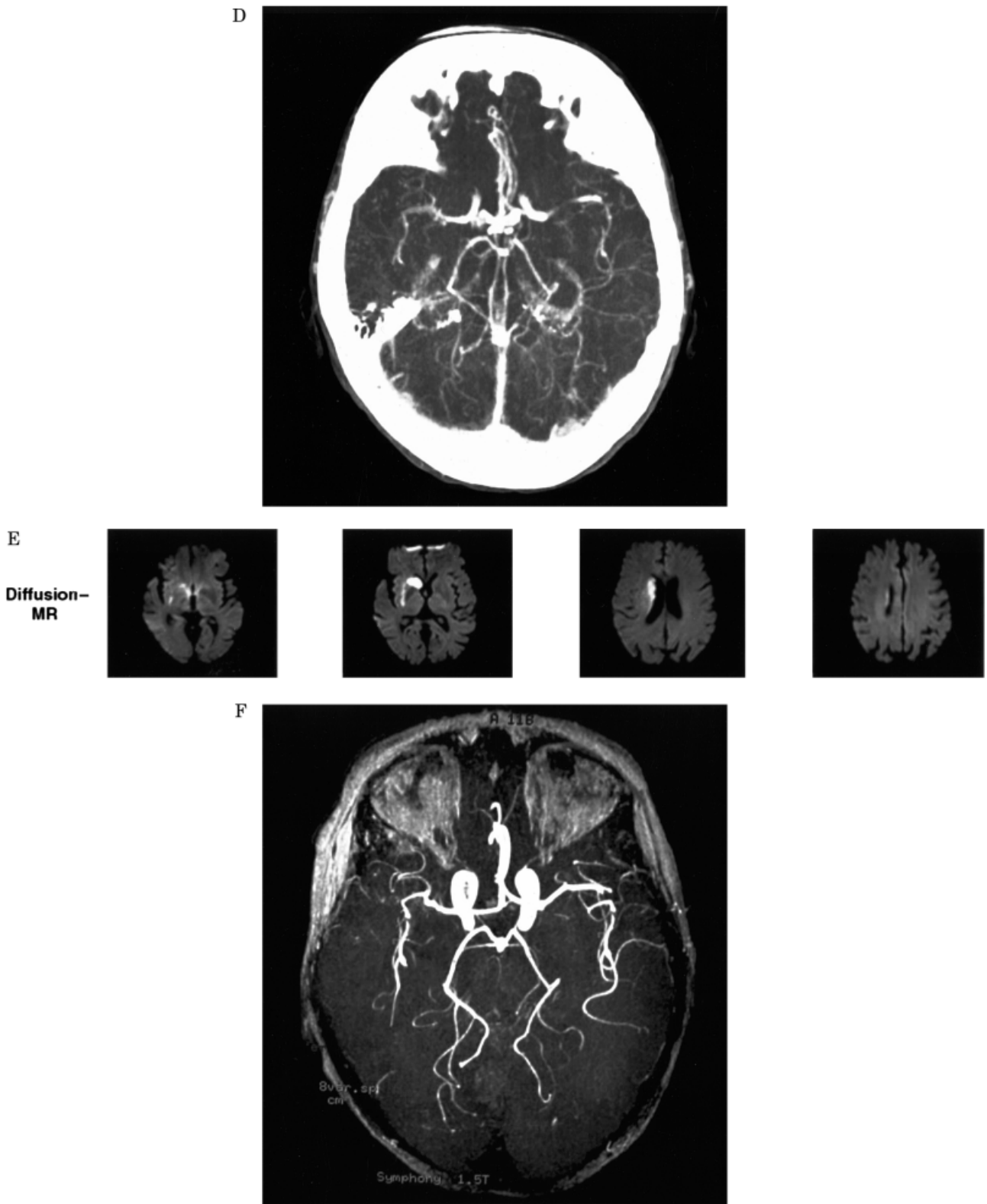


Figure 2 (Continued)

Table 2. Overview of NIHSS Evolution Over a Median of 1 Month (Interquartile Range, 0.825–1.625 Months) and of the Potential Recuperation Ratio in 22 Patients

Arterial Recanalization Status	Thrombolysis	No Thrombolysis
Arterial recanalization	5 patients (+ 1 death) Time to hospital admission = 1.5 (1.125–1.5) hours ^a Time to thrombolysis = 3 (2.75–3) hours ^a PRR = 81% ± 16% ^b NIHSS improvement = 74% ± 20% ^b	8 patients Time to hospital admission = 3.75 (2.25–4.875) hours ^a PRR = 71% ± 11% ^b NIHSS improvement = 62% ± 20% ^b
No arterial recanalization	2 patients Time to hospital admission = 2 (2–2) hours ^a Time to thrombolysis = 2.725 (2.625–2.825) hours ^a PRR = 69% ± 15% ^b NIHSS improvement = 55% ± 19% ^b	6 patients Time to hospital admission = 6 (4–7.5) hours ^a PRR = 60% ± 12% ^b NIHSS improvement = 42% ± 12% ^b

^aTime delays are expressed as the median and interquartile range.

^bPercentages are expressed as the mean ± standard deviation.

PRR = potential recuperation ratio; NIHSS = clinical condition of patients, measured with the National Institutes of Health Stroke Scale.

Arterial Recanalization or Persistent Arterial Occlusion

In the 8 patients who underwent admission angio-CT, the procedure demonstrated an occluded cerebral artery. The delayed angio-MR, performed on all 22 patients, allowed evaluation of potential recanalization of the occluded cerebral artery, which occurred either spontaneously or as a result of thrombolytic therapy (Table 2). In 8 patients (2 patients in the thrombolysis group and 6 in the nonthrombolysis group), angio-MR demonstrated persistence of arterial occlusion. Of the 8

patients with an occluded artery on the admission angio-CT, 5 showed recanalization on the delayed angio-MR, whereas 3 showed persistent occlusion.

Correlation between Admission Perfusion Computed Tomography and Delayed Diffusion-Weighted Magnetic Resonance Results

In patients with a persistent occluded cerebral artery on the delayed angio-MR (Figs 1 and 3), the mean size of the ischemic lesion (infarct + penumbra) on the admission perfusion CT was $37.8 \pm 15.5 \text{ cm}^2$ (mean ±

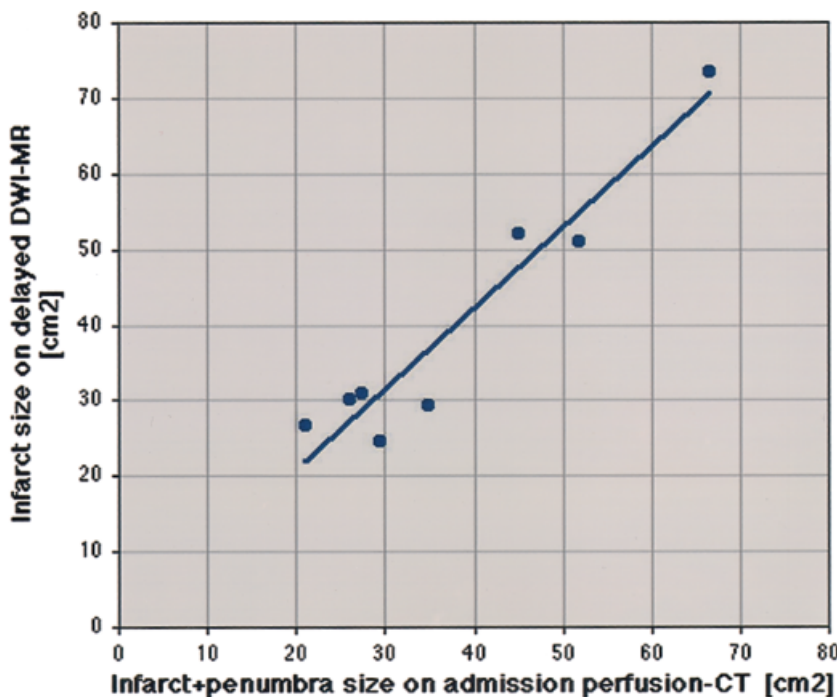


Fig 3. Relationship between ischemic lesion sizes on the perfusion computed tomography (CT) performed at the time of emergency room admission and delayed diffusion-weighted magnetic resonance (DWI-MR) in acute stroke patients without arterial recanalization. In patients with persistent arterial occlusion, the size of the cerebral infarct on the delayed DWI-MR strongly correlated ($DWI-MR^{infarct} = 3.659 + 0.861 \times \text{perfusion CT}^{infarct + penumbra}$; $r = 0.958$, $p < 0.001$) and showed no statistically significant difference ($p = 0.332$) with the size of the total ischemic area on the admission perfusion CT. In these patients, the penumbra defined on the admission perfusion CT gradually evolved towards infarct, with the entire cerebral ischemic area gradually becoming infarct, due to the prolongation of the arterial occlusion, thus explaining the observed distribution.

standard deviation), whereas the mean size of the infarct on the delayed DWI-MR series was $39.7 \pm 17.3 \text{ cm}^2$. No significant difference was seen between these significantly correlated values ($_{\text{DWI-MR}}\text{infarct} = 3.659 + 0.861 \times \text{perfusion}_{\text{CT}}\text{infarct} + \text{penumbra}$; correlation coefficient = 0.958; $p < 0.001$).

In all patients with a recanalized cerebral artery on the delayed angio-MR (Figs 2 and 4), the cerebral infarct on the delayed DWI-MR (mean \pm standard deviation, $21.3 \pm 18.6 \text{ cm}^2$) was larger than or the same size as the infarct on the admission perfusion CT ($12.0 \pm 11.1 \text{ cm}^2$), but smaller than or the same size as the ischemic lesion on the admission perfusion CT ($41.3 \pm 12.7 \text{ cm}^2$). Infarct size on the delayed DWI-MR was, on average, 22.6% of the range defined by the admission perfusion CT. Infarct sizes on the admission perfusion CT and on the delayed DWI-MR were significantly correlated ($_{\text{DWI-MR}}\text{infarct} = -0.568 \pm 0.753 \times \text{perfusion}_{\text{CT}}\text{infarct}$; $r = 0.926$; $p < 0.001$).

In patients with either arterial recanalization or persistent occlusion, the shape of the infarct or infarct-penumbra areas was similar on perfusion CT and DWI-MR images, as demonstrated in Figures 1 and 2.

Correlation between Perfusion Computed Tomography Results and Clinical Condition

The admission NIHSS increased with the initial size of the combined infarct and penumbra areas on the admission perfusion CT ($_{\text{admission}}\text{NIHSS} = 5.953 + 0.222 \times \text{perfusion}_{\text{CT}}\text{infarct} + \text{penumbra}$; $r = 0.627$;

$p = 0.002$) (Fig 5). However, there was no significant correlation between the size of the final cerebral infarct, as defined on the delayed DWI-MR, and the delayed NIHSS ($r = 0.587$; $p = 0.054$), Barthel index ($r = 0.302$; $p = 0.171$), or modified Rankin score ($r = 0.538$; $p = 0.114$).

Finally, the PRR was distributed as follows (see Table 2): In 6 patients in whom thrombolysis was not performed and the delayed angio-MR revealed a persistent occluded cerebral artery, the NIHSS improvement was $42 \pm 12\%$ (mean \pm standard deviation) and the PRR $60 \pm 12\%$. In 8 patients in whom thrombolysis was not performed and arterial recanalization was diagnosed on the delayed angio-MR, the NIHSS improvement was $62 \pm 20\%$ and the PRR $71 \pm 11\%$. In 5 patients in whom thrombolysis was performed and resulted in recanalization, the NIHSS improvement was $74 \pm 20\%$ and the PRR $81 \pm 16\%$. In 2 patients in whom thrombolysis was performed but did not result in arterial recanalization, the NIHSS improvement was $55 \pm 19\%$ and the PRR amounted to $69 \pm 15\%$.

Of the patients who underwent thrombolysis, a lower but nonsignificant NIHSS improvement of $55\% \pm 19\%$ was seen in those with a persistent occluded cerebral artery compared with those with recanalization ($74\% \pm 20\%$) ($p = 0.354$). This was associated with a lower but nonsignificant PRR ($p = 0.297$).

In patients with recanalization of the occluded cerebral artery, either spontaneous or consecutive to thrombolysis, there was a strong correlation between

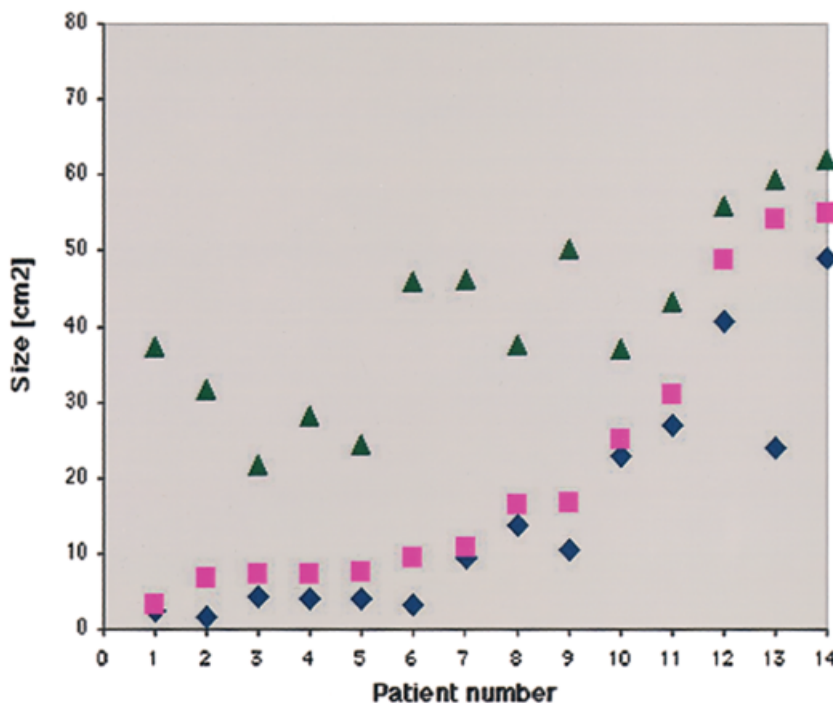


Fig 4. Correlation between ischemic lesion sizes on the admission perfusion computed tomography (CT) and delayed diffusion-weighted magnetic resonance (DWI-MR) in acute stroke patients with arterial recanalization. In all patients with a recanalized cerebral artery on the delayed angio-MR, the size of the final cerebral infarct defined on the delayed DWI-MR was larger than or the same size as the infarct on the admission perfusion CT, but smaller than or the same size as the ischemic lesion on the admission perfusion CT. This was probably related to the evolution of the infarct over the penumbra as defined on the admission perfusion CT until arterial recanalization occurred, followed by recovery of the remaining penumbra. \blacklozenge Infarct on admission perfusion-CT; \blacksquare infarct on delayed DWI-MR; \blacktriangle infarct + penumbra on admission perfusion-CT.

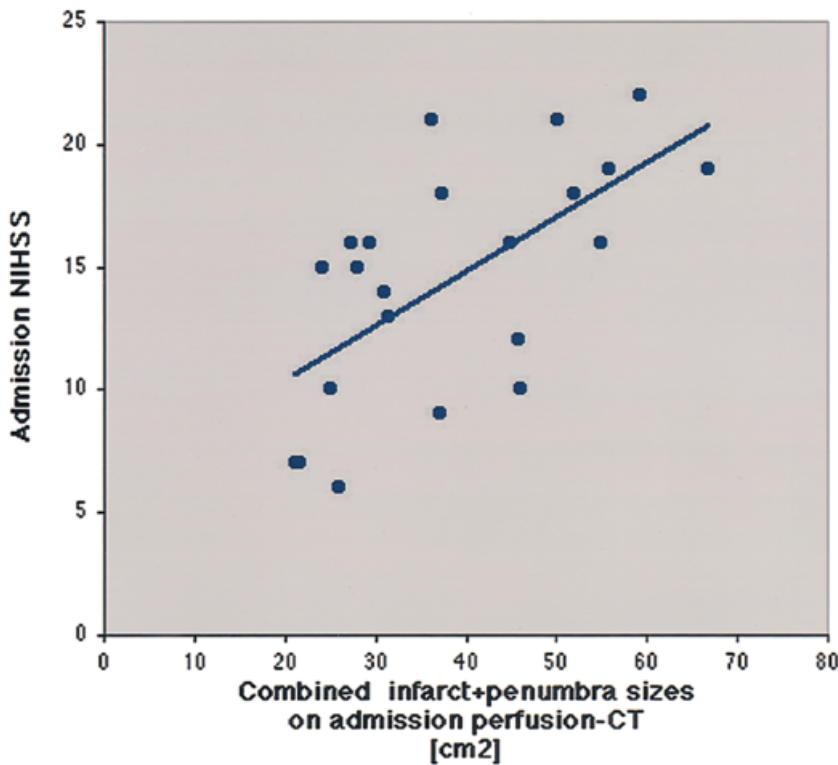


Fig 5. Correlation between the clinical condition of patients at the time of emergency room admission, measured with the National Institutes of Health Stroke Scale (NIHSS), and combined infarct-penumbra size on the admission perfusion computed tomography (CT) ($r = 0.627$, $p = 0.002$). The admission NIHSS increased concomitantly with the initial size of the combined infarct and penumbra areas on the admission perfusion CT ($_{admission} NIHSS = 5.953 + 0.222 \times_{perfusion-CT} infarct + penumbra$); the more extensive the initial ischemic cerebral area, the worse the clinical condition, especially on admission. At later clinical time points, neural repair and neuroplasticity allowed various degrees of improvement to occur in different patients, explaining the poorer correlation between the size of the cerebral infarct by delayed diffusion-weighted magnetic resonance (DWI-MR) and the clinical scores.

the PRR and the improvement in the NIHSS evaluated on admission and after a median of 1 month (interquartile range, 0.825–1.625 months) (NIHSS im-

provement = $0.108 + 0.863 \times_{perfusion\ CT} PRR$; $r = 0.833$; $p = 0.001$; Fig 6).

In patients with a persistent occluded cerebral artery,

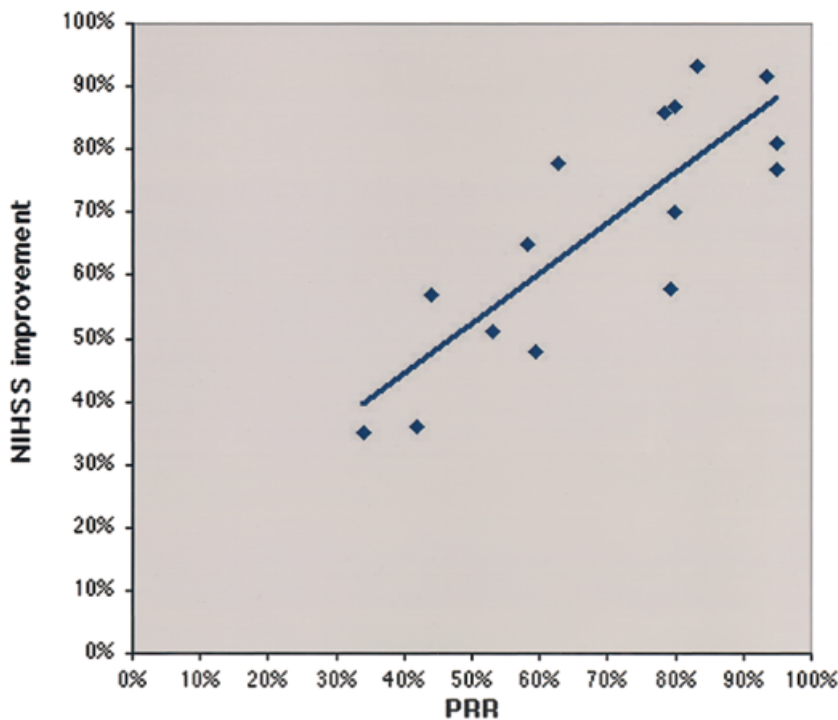


Fig 6. Correlation between the potential recuperation ratio (PRR) and improvement in clinical condition measured with the National Institutes of Health Stroke Scale (NIHSS) in acute stroke patients with arterial recanalization. In patients with recanalization of the occluded cerebral artery, there was a strong correlation between the PRR and improvement in the NIHSS evaluated on admission and after a median delay of 1 (interquartile range, 0.825–2.625 months) (NIHSS improvement = $0.108 + 0.863 \times_{perfusion\ CT} PRR$; $r = 0.833$, $p = 0.001$). In these patients, recanalization, whether spontaneous or after thrombolysis, allowed the penumbra to be salvaged, with subsequent proportional improvement in the patients' clinical condition.

the NIHSS improvement was globally poorer ($45 \pm 15\%$; mean \pm standard deviation) than in the recanalization group ($67 \pm 20\%$) ($p = 0.059$), and the PRR significantly lower ($60 \pm 12\%$ vs $71 \pm 11\%$; $p = 0.005$). In the persistent occlusion group, there was no correlation between NIHSS improvement and PRR (NIHSS improvement = $0.769 - 0.106 \times \text{perfusion CT-PRR}$; $r = 0.111$; $p = 0.859$).

Discussion

Perfusion CT examinations are not time-consuming, since they can be integrated into the cerebral CT survey performed on every stroke patient, and are well tolerated.²⁴ In most hospitals, CT units are available 24 hours a day, 7 days a week. The intravenous administration of nonionic iodinated contrast material involved is easily performed, even in acute stroke patients.⁴⁵

The radiation dose in a perfusion CT study is equivalent to that in a standard cerebral CT examination. For the acquisition of four adjacent 10mm sections at 80kVp, the measured normalized and weighted CT dose index (nCTDIw) amounts to 0.112mGy/mAs. For a perfusion CT protocol of 40 successive slices performed in cine mode at 100mA and with the geometry of radiation delivery on the Lightspeed CT unit (dose efficiency of 86%), the radiation dose amounts to 368mGy. To estimate the stochastic effect of the radiation, these doses must be distributed over the entire brain. Since a 40mm thickness ($4 \times 10\text{mm}$ sections) is approximately equal to one-fifth of the whole cerebral size, the absorbed dose to the brain is 77mGy. Using a weighting factor of 0.0023mSv/(mGy \times cm) for the brain, the cerebral effective dose is 3.4mSv, which is quite similar to the dose level for a standard cerebral CT examination (2.5mSv).^{44,46,47}

Perfusion CT examination with data analysis according to the central volume principle⁴⁸ allows accurate quantitative assessment of both the rCBF and the rCBV²⁴ as well as definition of the cerebral infarct and penumbra, as described above. Our proposed method for the calculation of cerebral penumbra and infarct maps from the rCBF and rCBV maps provided by perfusion CT data analysis relies on (1) the reported rCBF threshold of ischemia and (2) preserved (penumbra) or altered (infarct) autoregulatory mechanisms. In the penumbra, the rCBV is greater than 2.5ml per 100g, whereas in the infarcted area it is less. In agreement with the values most frequently reported in the literature,^{13,19,20,49–51} we arbitrarily chose a relative rCBF cutoff of 34% and an absolute rCBV cutoff of 2.5ml per 100g as indicative of ischemic brain and of cerebral parenchyma highly likely to die, respectively.

Although the MTT is affected at an earlier stage by cerebral ischemia, it is less specific and we therefore chose an rCBF threshold, rather than an MTT thresh-

old, to determine the total ischemic area (infarct and penumbra). Indeed, soon after the onset of ischemia, the MTT is prolonged and the rCBV is increased as a result of cerebral vascular autoregulation. If both increase by the same proportion, the rCBF, which is equal to the rCBV divided by the MTT, is unchanged, and thus there is no real cerebral parenchymal damage.

Correlation between Admission Perfusion Computed Tomography and Delayed Diffusion-Weighted Magnetic Resonance Results

In terms of the comparison between admission perfusion CT and delayed DWI-MR, our results underscore the excellent prognostic value of admission perfusion CT as regards the final size of the cerebral infarct, defined by reference DWI-MR sequences. As explained above, DWI-MR has been shown to accurately delineate the cerebral infarct.^{5,8,52} In order to avoid pitfalls related to biphasic phenomena,^{39,40} we chose to use the DWI-MR results obtained at a median of 3 days (interquartile range, 3–4 days) after stroke as a reference.

Eight of the 22 acute stroke patients showed persistent arterial occlusion, and in 2 of them thrombolytic therapy was unsuccessful. In these patients with persistent arterial occlusion, the penumbra defined on the admission perfusion CT gradually evolved towards infarct; due to prolongation of the arterial occlusion, the entire cerebral ischemic area became infarcted with time (see Fig 2). Thus, the size of the combined cerebral infarct and penumbra on the admission perfusion CT and the size of the cerebral infarct on the delayed MR were closely correlated and not statistically different (see Fig 4).

Fourteen of our 22 acute stroke patients showed recanalization of the occluded cerebral artery; 6 of them had received thrombolytic therapy, while recanalization was spontaneous in the other 8 patients. In patients with recanalization of the occluded cerebral artery (see Fig 3), the cerebral infarct on the delayed DWI-MR was larger than or the same size as the infarct on the admission perfusion CT, but smaller than or the same size as the ischemic lesion on the admission perfusion CT. More precisely, its average was located at 22.6% of the range defined by the sizes of the cerebral infarct and ischemia on the admission perfusion CT. This was probably due to the gradual replacement of the penumbra by infarct (particularly marked in Patient 13; see Fig 4) until arterial recanalization, followed by recovery of the remaining penumbra (see Fig 1). Significant correlation was identified between the infarct sizes on the admission perfusion CT and on the delayed DWI-MR, in agreement with a previous report of patients with documented recanalization during intra-arterial thrombolysis.⁵³

Two objections could be raised to our study proto-

col. First, the four examined cerebral slices were not exactly the same in the perfusion CT and DWI-MR, as there was an interval of several days between the two examinations. However, for each patient, we performed an averaging of the ischemic areas calculated on four adjacent slices, thus decreasing the inaccuracy due to the same slices not being used. Second, the precise moment of recanalization of the occluded cerebral artery could not be accurately determined from the admission perfusion CT and delayed DWI-MR. However, it was impossible to repeat the imaging examinations of all the acute stroke patients, the exceptions being those cases in which clinical evolution made it mandatory (see Figs 1 and 2).

Finally, our choice of cerebral DWI-MR as the reference for the final infarct size is justified by reports of its accuracy in the delineation of the nature and size of brain ischemia and the quantification of tissue in moderate-to-advanced stages of injury.^{5,8,52,54-57} We decided to use delayed DWI-MR in order to avoid controversy related to biphasic phenomena, which were reported during the early phase after stroke.^{39,40} We did not evaluate the use of perfusion MR, which only allows semiquantitative assessment of rCBF,⁵⁸ preventing the use of thresholds.

Correlation between Perfusion Computed Tomography Results and Patients' Clinical Condition

In the first part of the study, we demonstrated a correlation between the ischemic cerebral areas estimated by two imaging techniques, the reference method (DWI-MR) and the method to be validated (perfusion-CT). In the second part, we wished to evaluate the clinical relevance of perfusion CT examinations performed on admission in acute stroke patients. Three clinical scores, the NIHSS, Barthel index, and modified Rankin scale, all proven to give an assessments of clinical condition,⁴¹⁻⁴² were used. In addition, we examined the evolution of the NIHSS between admission and a median of 1 month (interquartile range, 0.825-1.625 months) later.

A good correlation was found between the admission NIHSS and the initial size of the combined cerebral infarct and penumbra defined on the admission perfusion CT (see Fig 5), while a poor correlation was found between the delayed DWI-MR size of the cerebral infarct and the various clinical scores. The most likely explanation for this poorer correlation between DWI-MR lesion size and delayed clinical score is that the results of an MR examination on day 3 (interquartile range, 3-4 days) were compared with the clinical scores at a median of 1 month (interquartile range, 0.825-1.625 months), rather than with the clinical scores on day 3, neural repair and neuroplasticity allowing variable amounts of improvement in different patients at the later clinical time points.

Finally, we evaluated a new parameter, PRR, which is the ratio of the size of the penumbra to the size of the penumbra plus infarct, as a means of predicting improvement in the NIHSS between admission and after a median of 1 month (interquartile range, 0.825-1.625 months) (see Table 2 and Fig 6).

In 14 patients, thrombolysis was not performed. In 8 of these, spontaneous fragmentation of the thrombus with recanalization of the occluded cerebral artery occurred, as demonstrated by the delayed angio-MR, while in 6 no arterial recanalization occurred. In the latter group, clinical evolution was not as good, reflected by the lower NIHSS improvement and PRR.

Thrombolysis was performed on 8 patients, allowing recanalization of the arterial thrombus and salvaging the penumbra in 6,¹⁰ this being reflected by the high NIHSS improvement of $74 \pm 20\%$ (mean \pm standard deviation). In the remaining 2 patients, thrombolysis was unsuccessful, as reflected by the NIHSS improvement of only $55 \pm 19\%$ and the lower PRR of $69 \pm 15\%$.

In patients with recanalization of the occluded cerebral artery, whether spontaneous or with thrombolysis, there was a strong correlation between the PRR and the improvement in the NIHSS evaluated on admission and after a median of 1 month (interquartile range, 0.875-1.625 months) (see Fig 6). In these patients, recanalization allowed the penumbra to be salvaged, with a subsequent and proportional improvement in clinical condition.

In patients with a persistent occluded cerebral artery, the cerebral infarct gradually evolved over the penumbra and finally completely replaced it, as reflected by a globally poorer NIHSS improvement. Since the PRR is calculated from the sizes of the penumbra and infarct on admission, it is significant when the penumbra recovers (as with arterial recanalization) and allows clinical improvement. On the other hand, it showed no correlation with NIHSS improvement in the persistent occlusion group.

Since the PRR is computed based on the admission imaging survey, it should be independent of whether arterial recanalization occurs or not. Our data showing a substantially lower PRR in the persistent occlusion group suggests that infarcts were more mature in this group. This could be among the reasons why patients without arterial recanalization did not improve and showed globally poorer NIHSS improvement.

Conclusions

Perfusion CT examinations were performed on four adjacent 10mm cerebral sections in 22 patients with acute stroke in the cerebral artery territory. This procedure allowed accurate prediction of the final cerebral infarct size in acute stroke patients at the time of emergency evaluation and provided information about the

extent of the penumbra. The relationship between the perfusion CT abnormality and the final infarct size was shown to vary in a predictable fashion, depending upon whether arterial recanalization occurred. Perfusion CT accuracy was demonstrated by comparison with the results of delayed DWI-MR examinations.

Perfusion CT results correlate with the patients' clinical condition, the admission NIHSS being directly related to the size of the ischemic cerebral area on the admission perfusion CT. On the other hand, the delayed clinical scores are strongly influenced by neural repair and neuroplasticity, which allow various extents of improvement in different patients. Perfusion CT can be used to estimate a PRR, which is an indicator of the maturity of arterial occlusion and cerebral infarct and which correlates with evolution of the NIHSS in patients with arterial recanalization.

Even if these conclusions need to be confirmed in larger series, this article shows perfusion CT examination to be a valuable tool in the early evaluation of acute stroke patients and possibly in the selection of the therapeutic strategy.

We thank Mrs M Rousselle and Mr T Barkas for their help in editing this manuscript.

References

- National Institute of Neurological Disorders and Stroke (NINDS) rt-PA Stroke Study Group. Tissue plasminogen activator for acute ischaemic stroke. *N Engl J Med* 1995;33: 1581–1587.
- Bogousslavsky J, Van Melle G, Regli F. The Lausanne stroke registry: analysis of 1,000 consecutive patients with first stroke. *Stroke* 1988;19:1083–1092.
- Hennerici M. Improving the outcome of acute stroke management. *Hosp Med* 1999;60:44–49.
- Hacke W, Kaste M, Fieschi C. Randomised double-blind trial placebo-controlled trial of thrombolytic therapy with intravenous therapy with intravenous alteplase in acute ischaemic stroke (ECASS II). *Lancet* 1998;352:1245–1251.
- Oppenheim C, Samson Y, Manai R, et al. Prediction of malignant middle cerebral artery infarction by diffusion-weighted imaging. *Stroke* 2000;31:2175–2185.
- Rubin G, Firlirk AD, Levy EI, et al. Relationship between cerebral blood flow and clinical outcome in acute stroke. *Cerebrovasc Dis* 2000;10:298–306.
- Karonen JO, Nuutinen J, Kuikka JT, et al. Combined SPECT and diffusion-weighted MRI as predictor of infarct growth in acute ischemic stroke. *J Nucl Med* 2000;41:788–794.
- Sorensen AG, Copen WA, Ostergaard L, et al. Hyperacute stroke: simultaneous measurement of relative cerebral blood volume, relative cerebral blood flow, and mean tissue transit time. *Radiology* 1999;210:519–527.
- Ezura M, Takahashi A, Yoshimoto T. Evaluation of regional cerebral blood flow using single photon emission tomography for the selection of patients for local fibrinolytic therapy of acute cerebral embolism. *Neurosurg Rev* 1996;19:231–236.
- Heiss WD, Grond M, Thiel A, et al. Ischemic brain tissue salvaged from infarction with alteplase. *Lancet* 1997;349: 1599–1600.
- Reivich M. Blood flow metabolism couple in brain. *Res Pub Assoc Res Nerv Ment Dis* 1974;53:125–140.
- Lassen NA. Cerebral blood flow and oxygen consumption in man. *Physiol Rev* 1959;39:183–238.
- Hossmann KA. Viability thresholds and the penumbra of focal ischemia. *Ann Neurol* 1994;36:557–565.
- Symon L, Branston NM, Strong AJ, Hope TD. The concepts of thresholds of ischaemia in relation to brain structure and function. *J Clin Pathol* 1977;30(Suppl):149–154.
- Astrup J, Symon L, Siesjö BK. Thresholds in cerebral ischemia: the ischemic penumbra. *Stroke* 1981;12:723–725.
- Hakim AM. The cerebral ischemic penumbra. *Can J Neurol Sci* 1987;14:557–559.
- Hossmann KA. Neuronal survival and revival during and after cerebral ischemia. *Am J Emerg Med* 1994;1:191–197.
- Heiss WD. Ischemic penumbra: evidence from functional imaging in man. *J Cereb Blood Flow Metab* 2000;20:1276–93.
- Harper AM. Autoregulation of cerebral blood flow: influence of the arterial blood pressure on the blood flow through the cerebral cortex. *J Neurol Neurosurg Psychiatry* 1966;29:398–403.
- Wood JH. Cerebral blood flow: physiologic and clinical aspects. New York: McGraw-Hill, 1987.
- Symon L, Ganz JC, Dorsch NWC. Experimental studies of hyperaemic phenomena in the cerebral circulation of primates. *Brain* 1972;95:265–278.
- Gourley JK, Heistad DD. Characteristics of reactive hyperemia in the cerebral circulation. *Am J Physiol* 1984;246 (Heart Circ Physiol 15):H52–H58.
- Todd NV, Picozzi P, Crockard HA. Quantitative measurement of cerebral blood flow and cerebral blood volume after cerebral ischemia. *J Cereb Blood Flow Metab* 1986;6:338–341.
- Wintermark M, Maeder P, Thiran J-Ph, et al. Simultaneous measurements of regional cerebral blood flows by perfusion-CT and stable xenon-CT: a validation study. *AJNR* 2001;22: 905–914.
- Nabavi DG, Cenic A, Craen RA, et al. CT assessment of cerebral perfusion: experimental validation and initial clinical experience. *Radiology* 1999;213:141–149.
- Cenic A, Nabavi DG, Craen RA, et al. Dynamic CT measurement of cerebral blood flow: a validation study. *AJNR Am J Neuroradiol* 1999;20:63–73.
- König M, Klotz E, Luka B, et al. Perfusion CT of the brain: diagnostic approach for early detection of ischemic stroke. *Radiology* 1998;209:85–93.
- Meier P, Zierler KL. On the theory of the indicator-dilution method for measurement of blood flow and size. *J Appl Physiol* 1954;12:731–744.
- Zierler KL. Theoretical basis of indicator-dilution methods for measuring flow and size. *Circ Res* 1962;10:393–407.
- Zierler KL. Equations for measuring blood flow by external monitoring of radioisotopes. *Circ Res* 1965;16:309–321.
- Axel L. Cerebral blood flow determination by rapid-sequence computed tomography. *Radiology* 1980;137:679–686.
- Axel L. A method of calculating brain blood flow with a CT dynamic scanner. *Adv Neurol* 1981;30:67–71.
- Axel L. Tissue mean transit time from dynamic computed tomography by a simple deconvolution technique. *Invest Radiol* 1983;18:94–99.
- Ladurner G, Zilkha E, Iliff LD, et al. Measurement of regional cerebral blood volume by computerized axial tomography. *J Neurol Neurosurg Psychiatry* 1976;39:152–155.
- Zilkha E, Ladurner G, Linette D, et al. Computer subtraction in regional cerebral blood-size measurements using the EMI-scanner. *Br J Radiol* 1976;49:330–334.
- Ladurner G, Zilkha E, Sager WD, et al. Measurement of regional cerebral blood volume using the EMI 1010 scanner. *Br J Radiol* 1979;52:371–374.

37. Larson OA, Lassen NA. Cerebral hematocrit in normal man. *J Appl Physiol* 1964;19:571–574.
38. Sakai F, Kakazawa K, Tazaki Y, et al. Regional cerebral blood volume and hematocrit measured in human volunteers by single-photon emission tomography. *J Cereb Blood Flow Metab* 1985;5:207–213.
39. Miyasaka N, Nagaoka T, Kuroiwa T, et al. Histopathologic correlates of temporal diffusion changes in a rat model of cerebral hypoxia/ischemia. *AJNR Am J Neuroradiol* 2000;21:60–66.
40. Oppenheim C, Stanescu R, Dormont D, et al. False-negative diffusion-weighted MR findings in acute ischemic stroke. *AJNR Am J Neuroradiol* 2000;21:1434–1440.
41. Williams LS, Yilmaz EY, Lopez-Yunez AM. Retrospective assessment of initial stroke severity with the NIH Stroke Scale. *Stroke* 2000;31:858–862.
42. Adams HP Jr, Davis PH, Leira EC, et al. Baseline NIH Stroke Scale score strongly predicts outcome after stroke: a report of the Trial of Org 10172 in Acute Stroke Treatment (TOAST). *Neurology* 1999;53:126–131.
43. DeGraba TJ, Hallenbeck JM, Pettigrew KD, et al. Progression in acute stroke: value of the initial NIH stroke scale score on patient stratification in future trials. *Stroke* 1999;20:1208–1212.
44. Wintermark M, Maeder P, Verdun FR, et al. Using 80 kVp versus 120 kVp in perfusion CT measurement of regional cerebral blood flows. *AJNR Am J Neuroradiol* 2000;21:1881–1884.
45. Doerfler A, Engelhorn T, von Kummer R, et al. Are iodinated contrast agents detrimental in acute cerebral ischemia? An experimental study in rats. *Radiology* 1998;206:211–217.
46. Commission of the European Communities. European guidelines on quality criteria for computed tomography. EUR 16262 EN, 1999. Available from: URL:<http://www.drs.dk/guidelines/ct/quality/>
47. Hidajat N, Mäurer J, Schröder RJ, et al. Relationships between physical dose quantities and patient dose in CT. *Br J Radiol* 1999;72:556–561.
48. Wintermark M, Maeder P, Thiran J-Ph, Schnyder P, Meuli R. Quantitative assessment of regional cerebral blood flows by perfusion CT studies at low injection rates: a critical review of the underlying theoretical models. *Eur Radiol* 2001;11:1220–1230.
49. Mayer TE, Hamann GF, Baranczyk J, et al. Dynamic CT perfusion imaging of acute stroke. *AJNR Am J Neuroradiol* 2000;21:1441–1449.
50. Hunter GJ, Hamberg LM, Ponzo JA, et al. Assessment of cerebral perfusion and arterial anatomy in hyperacute stroke with three-dimensional functional CT: early clinical results. *AJNR Am J Neuroradiol* 1998;19:29–37.
51. Lee KH, Soo-Jin C, Byun HS, et al. Triphasic perfusion computed tomography in acute middle cerebral artery stroke: a correlation with angiographic findings. *Arch Neurol* 2000;57:990–999.
52. Gonzales RG, Schaefer PW, Buonanno FS, et al. Diffusion-weighted MR imaging: accuracy in patients imaged within 6 hours of stroke symptom onset. *Radiology* 1999;210:155–162.
53. Lev MH, Segal AZ, Farkas J, et al. Utility of perfusion-weighted CT imaging in acute middle cerebral artery stroke treated with intra-arterial thrombolysis: prediction of final infarct volume and clinical outcome. *Stroke* 2001;32:2021–2028.
54. Kluytmans M, Van Everdingen KJ, Kappelle LJ, et al. Prognostic value of perfusion- and diffusion-weighted MR imaging in first 3 days of stroke. *Eur Radiol* 2000;10:1434–1441.
55. Kim JH, Lee SJ, Kang KH, et al. Correlative assessment of hemodynamic parameters obtained with T2*-weighted perfusion MR imaging and SPECT in symptomatic carotid artery occlusion. *AJNR Am J Neuroradiol* 2000;21:1450–1456.
56. Smith AM, Grandin CB, Duprez T, et al. Whole brain quantitative CBF, CBV, MTT measurements using MRI bolus tracking: implementation and application to data acquired from hyperacute stroke patients. *J Magn Reson Imag* 2000;12:400–410.
57. Lythgoe MF, Thomas DL, Calamante F, et al. Acute changes in MRI diffusion, perfusion, T1, and T2 in a rat model of oligemia produced by partial occlusion of the middle cerebral artery. *Magn Reson Med* 2000;44:706–712.
58. Sorensen AG, Reimer P. Cerebral MR perfusion imaging: principles and current applications. Stuttgart: Thieme Verlag, 2000.